Chapter 5

Conclusion and Outlook

5.1 Introduction

In this thesis, we have addressed three different problems in low dimensional condensed matter physics. The first one is a field theoretic treatment of the magnetic properties of charged spinless Bosons. The second one concerns the disordered electronic states in an external magnetic field. And the third is interface growth in a random porous medium. In this final chapter, we would like to highlight some features of these problems and indicate some possible extensions.

5.2 Diamagnetism of Charged Spinless Bosons

In chapter 1, we have reviewed the magnetic properties of charged particles as background for our work described in chapter 2. In particular, we have described the original proof of diamagnetism of spinless Bosons. We observe that the free energy of spinless Bosons in an external magnetic field is higher than the free energy without the magnetic field. This diamagnetism is a universal property of spinless Bosons in the sense that it holds regardless of whether the external magnetic field is homogeneous or inhomogeneous or whether the system is interacting or non-interacting. This proof is a *non-perturbative* one. In this chapter, we also review an alternative proof of this diamagnetic inequality. This alternative proof uses a connection between Brownian motion and magnetism. The inequality follows from an interesting

relation between the area distribution in a Brownian motion and the partition function of a magnetic system. The magnetic field is used here as a counter to measure the area enclosed in Brownian motion.

In chapter 2, we have done a field theoretic generalization of the diamagnetism of spinless Bosons. In the first part, we have discussed the response of free charged scalar fields in an external constant magnetic field in two dimensions. Here, we have used mode matching to regularize the divergent free energy. We have shown that the difference between the free energy with and without the magnetic field is *finite,* cut-off *independent* and *positive* definite.

In the interacting case it turns out that the partition function and hence the free energy cannot be evaluated in closed form but still one can show the diamagnetism of charged scalar fields. We have integrated out only those field configurations which are within a sphere of fixed radius in the momentum space. The interaction between the scalar fields $V(\Phi^*\Phi)$ is gauge invariant. We have suitably redefined the measure of the integral through the inclusion of self-interaction. This has the advantage that the effects of self-interaction and interaction via a dynamical EM field have been separated.

It is clear from the section on interacting case in chapter 2 that the proof of diamagnetic inequality is true for any dimension and independent of the self-interaction of the scalar field. The proof does not assume a specific form for the vector potential. This implies that the theory holds good even when the applied magnetic field is inhomogeneous.

The diamagnetism of spinless Bosons is relevant to current ideas on some of the macroscopic properties of Fractional Quantum Hall Effect [1] through the *Composite Bosons* idea [2, 3]. In this body of work, composite Bosons are formed by attaching an *odd* number of flux quanta to each electron. This mapping of interacting Fermions to Bosons generates a statistical gauge field proportional to density

of electrons in addition to the external magnetic field. An explanation of the Hall plateaus is sought in the Meissner effect of these Composite Bosons.

5.3 2d Disordered Tight-Binding Hamiltonian in a Magnetic Field

In chapter 3, we have discussed the eigenstates of a tight-binding Hamiltonian in an external magnetic field with on-site disorder. The classification of the eigenstates has been made by studying the GIPR and the multi-fractality of the eigenstates. We have looked here only the effect of disorder in the lowest energy eigenstate. It is also important from the point of view of Integer Quantum Hall Effect (IQHE) [1] to investigate the eigenstates in the center of the band. Characterizing this eigenstate will be useful in explaining the plateaus seen in the experiment. One can also investigate the effect of disorder and magnetic field on this eigenstate. Work in this direction is in progress, but not reported in this thesis.

In this tight-binding Hamiltonian, one can estimate the localization length exponent via multi-fractality. In a system of finite size, the localization length ξ of the electronic states is larger than the system size L for a certain range of energies $\Delta E(= E - E_c)$ around the critical energy E_c. In the thermodynamic limit,

$$\xi \sim |E - E_c|^{-\tilde{\nu}} \tag{5.1}$$

Without computing $\tilde{\nu}$ from the finite size scaling of Hall conductivity [4], one can use multi-fractal analysis **[5]** to estimate it. This will help us understand the fluctuations of the eigenstates around the critical energies. In that situation one is interested in looking at the q-th moment of the participation ratio as a function of the system size L and the distances from the critical energy E_c. One finds [5] for a fixed system size L,

$$\mathcal{P}(q, L, E) \sim |E - E_c|^{\pi(q)} \tag{5.2}$$

Using a finite size scaling ansatz, one finds

$$\mathcal{P}(q, L, E) \sim L^{-\tau(q)}\ F_q(L^{1/\tilde{\nu}}(E - E_c)) \tag{5.3}$$

The condition that $\mathcal{P}(q, L, E)$ is finite for $E \# E_c$ leads to the scaling relation

$$\pi(q) = \tilde{\nu}\tau(q) \tag{5.4}$$

In particular, for the inverse participation ratio, one finds

$$\pi(2) = \tilde{\nu}\ D_2 \tag{5.5}$$

Using $D_2 = 1.62 \pm 0.02$, Huckestein and Schweitzer [6] obtained 2.4 ± 0.3 in agreement with the result obtained from the finite size scaling of the localization length. It will also be interesting to look for an analytical calculation of this robust exponent $\tilde{\nu}$ starting from an appropriate disordered Hamiltonian.

5.4 Imbibition of Solution through Random Porous Medium

In chapter *3*, we have studied the Imbibition problem both from experiment and numerical simulation. From our experiment conducted under two conditions, we have found the roughness exponent to be different. We have introduced a discrete cellular automaton model to explain the different exponents obtained in experiments. This model gives rise to a set of tunable exponents. The discrete model also shows power law avalanches and multi-affinity of the interface.

5.4.1 On Experimental Aspects

Our cellular automaton model suggests that roughness exponents are not universal and depend on evaporation. It would be interesting to study experimentally the universality of the exponents. One can measure the roughness exponent of the growing interface in an experiment. However, it turns out that with this simple-minded

tabletop setup, it is difficult to measure the dynamic roughness of the interface. One has to digitize the image of the interface at consecutive time intervals and then measure the correlation between the heights at these two time intervals. The log-log plot of these correlations versus the time difference gives the dynamic exponent. This is the method which we have used to compute the dynamic exponent in our model.

Recently, employing this approach, Horvath and Stanley [7] have studied the growing interface during imbibition of viscous liquids in filter paper. They compute the height-height auto-correlation using a constant driving force and find $C(\tau) \sim \tau^{\beta}$ with $\beta = 0.56 \pm 0.03$. They also establish that the scaling of surfaces during roughening in the presence of quenched noise exhibits driving force independent scaling behaviour.

Another sophisticated way of characterizing the roughness of the interface is through the established dynamical scaling [8] of the growing interface by an image scanner with an appreciable resolution. In this method one computes the root mean square value of the height fluctuation defined by

$$w(L,t) = \left(< h^2 > - < h >^2 \right)^{1/2} \tag{5.6}$$

The average height is defined as $< h(L,\mathrm{t}) >= \frac{1}{L} \mathrm{X}\, h(x,\mathrm{t})$, where the summation extends over $x = 1, 2, ...\mathrm{L}$. This (global) width w is a measure of transverse correlation in the direction of growth. It was proposed by Family and Vicsek [8] that the width satisfies the following scaling relation

$$w(L,t) \sim L^{\alpha} f(t/L^{z}) \tag{5.7}$$

This relation has been verified in numerous simulations of the interface growth phenomenon. The dynamic exponent z is defined by $z = \alpha/\beta$. For $\mathrm{t} \ll L^{z}$, $w(L,\mathrm{t})$ reduces to

$$w(L,\mathrm{t}) \sim t^{\beta} \tag{5.8}$$

and, for t $\gg L^z$,

$$w(L,t) \sim L^{\alpha} \tag{5.9}$$

Thus, the average width $w(L,t)$ scales with time and the exponent β describes the growth of the width along the growth direction. This dynamic scaling approach is a useful means of describing fluctuations far from equilibrium which cannot be described in terms of equilibrium statistical mechanics. This approach has been recently employed in the study of a growing self-affine interface formed in a paper-towel-wetting experiment [9] with a red food dye solution.

5.4.2 On Theoretical Aspects

Since the model presented here is not a discretization of any continuum partial differential equation, it would be interesting to investigate the non-linearity in the model. This can be done by introducing a helicoidal boundary condition [10] which introduces a slope to the interface (m = Vh). In a discrete model, the helicoidal boundary condition is implemented by imposing $h(L,t) = h(1,t) - m(L-1)$. The nonlinearity of the corresponding continuum partial differential equation can be probed by studying the dependence of the front velocity. The velocity of the interface is computed from the heights measured at subsequent time intervals. The variation of this velocity with the slope m is plotted and fitted with some polynomial. The coefficients of terms higher than or equal to 2 in the polynomial determine the non-linearities in the model. It is also important to note the signs of the non-linear coefficients which can help in understanding the growth process of the interface.

It is known [11] that the KPZ equation has a Galilean invariance[1]. This invariance enforces a strict identity between the static and dynamic exponent given by $\alpha + z = 2$ provided the noise has no temporal correlation. This identity is true in any dimension. However, in most of the experiments and numerical simulations

[1]The transformation is defined by $h' = h + \epsilon x$, $x' = x - \lambda \epsilon t$, $t' = t$ and ϵ is the infinitesimal angle by which the interface has been tilted

(including DPD and ours), it is found that $a + z \neq 2$ (see Appendix B). This could be due to the quenched disorder present in the medium. (In that situation, the coefficient of the non-linear term is expected to be renormalized. It would be interesting to derive such an identity in case of quenched disordered model.)

We have studied the problem from a discrete cellular automaton model. There is another approach to the problem from a continuum partial differential equation. It would be interesting to formulate such a partial differential equation incorporating evaporation and quenched disorder explicitly. It would also serve as a starting point for a mean field approximation and for taking into account the effect of fluctuations systematically. One might also be able to develop some appropriate renormalization techniques. This will help in comparing the effect of evaporation on the roughness exponent with numerical and experimental observations. Work in this direction is in progress.

One can study the asymmetry of the height configuration through a quantity called skewness. The skewness is defined as

$$s = \frac{\langle (\mathrm{h} - \langle \mathrm{h} \rangle)^3 \rangle}{\langle (\mathrm{h} - \langle \mathrm{h} \rangle)^2 \rangle^{3/2}} \tag{5.10}$$

The angular brackets here denote an averaging over samples. A non-zero value of s establishes the asymmetric configurations under vertical reflection $\mathrm{h} \rightarrow -\mathrm{h}$. This implies that non-linear terms breaking the $\mathrm{h} \rightarrow -h$ symmetry must be present in the large scale description of the surface. In other words, it also reflects the true non-equilibrium model of the growth. One can also compute the effective fourth cumulant given by

$$Q = \frac{\langle (\mathrm{h} - \langle \mathrm{h} \rangle)^4 \rangle}{\langle (\mathrm{h} - \langle \mathrm{h} \rangle)^2 \rangle^2} - 3 \tag{5.11}$$

A non-zero value of Q signals the asymmetry of the rough interface. These two quantities s and Q help one identify the non-linear terms in the stochastic growth equation.

The existence of various universality classes is a powerful concept in modern statistical mechanics, since it allows us to understand the differences between various growth processes. The formulation of a continuum partial differential equation of the imbibition process taking into account the effect of evaporation will help one identify the universality class.

In practical situations, there are a large number of effects shaping the actual morphology of the interface. However, out of these there are only a few that actually determine the scaling exponents of the system. Identifying them allows us to reduce the problem to one of a few growth equations. In this fashion, a large number of seemingly unrelated phenomena may be seen to belong to the same universality class, even though there is no apparent connection between them.

Bibliography

[1] R. E. Prange and S. M. Girvin eds, The *Quantum Hall Effect* (Springer-Verlag, New York, 1986).

[2] S. C. Zhang, T. H. Hansson, S. A. Kivelson, Phys. Rev. Lett., 62, 82 (1989); S. C. Zhang, Int. J. Mod. Phys. B, 6, 25 (1992).

[3] S. Kivelson, D.-H. Lee, and S. C. Zhang, Scientific American, 274, 64 (1996).

[4] D. P. Arovas, R. N. Bhatt, F. D. M. Haldane, P. B. Littlewood and R. Rammal, Phys. Rev. Lett., 60, 619 (1988); Y. Huo and R. N. Bhatt, Phys. Rev. Lett., 68, 1375 (1992); K. Yang and R. N. Bhatt, Phys. Rev. Lett., 76, 1316 (1996).

[5] B. Huckestein, Rev. Mod. Phys., 67, 357 (1995).

[6] B. Huckestein and L. Schweitzer, Phys. Rev. Lett., 72, 713 (1994).

[7] V. K. Horváth and H. E. Stanley, Phys. Rev. E, 52, 5166 (1995).

[8] F. Family and T. Vicsek, J. Phys. A, 18, L75 (1985); F. Family, Physica A, 168, 561 (1990).

[9] T. H. Kwon, A. E. Hopkins and S. E. O'Donnell, Phys. Rev. E, 54, 685 (1996).

[10] L. A. N. Amaral, A. L. Barabási and H. E. Stanley, Phys. Rev. Lett., 73, 62 (1994); L. A. N. Amaral, A. L. Barabási, H. A. Makse and H. E. Stanley, Phys. Rev. E, 52, 4087 (1995).

[11] E. Medina, T. H. Hwa, M. Kardar and Y. -C. Zhang, Phys. Rev. **A, 39, 3053** (1989).

Appendix A

Diamagnetic behaviour of Dirac electrons in 2d in an external homogeneous magnetic field

In this appendix, we compute the renormalized energy difference of QED in an external homogeneous magnetic field. In case of QED vacuum in an external homogeneous magnetic field, the energy levels for spin-up and spin down states are given by

$$\omega_{l,\sigma} = \sqrt{m^2 + 2l\ eB},\ \omega_{l,-\sigma} = \sqrt{m^2 + (2l+2)\ eB} \tag{A.1}$$

In this case, equation (2.20) becomes

$$\Lambda^2 \ = \ (2L+1)eB \tag{A.2}$$

Therefore, the energy $E_0(B, \mathrm{L})$ in presence of the magnetic field becomes

$$E_0(B,L) = -\frac{eB\ A}{2\pi}\left[\sum_{l=0}^{L}\ \omega_{l,\sigma} + \sum_{l=0}^{L-1}\omega_{l,-\sigma}\right] \tag{A.3}$$

Note that there is a difference in sign relative to the vacuum energy in the spin zero case. This minus sign occurs because spin $1/2$ particles satisfy the anti-commutation relation rather than commutation relations [1, 2, 3]. The energy without the magnetic field is given by

$$\begin{aligned} E_0(0,\Lambda) \ &= \ -\ \frac{2A}{6\pi}\ \left[(\Lambda^2+m^2)^{\frac{3}{2}} - m^3\ \right] \\ &= \ -\ \frac{2A}{6\pi}\ \left[(2L+1)eB + m^2)^{\frac{3}{2}} - m^3\ \right] \end{aligned} \tag{A.4}$$

It can be easily shown by numerically plotting and comparing the two energies that

$$E_0(B,L) \geq E_0(0,L) \tag{A.5}$$

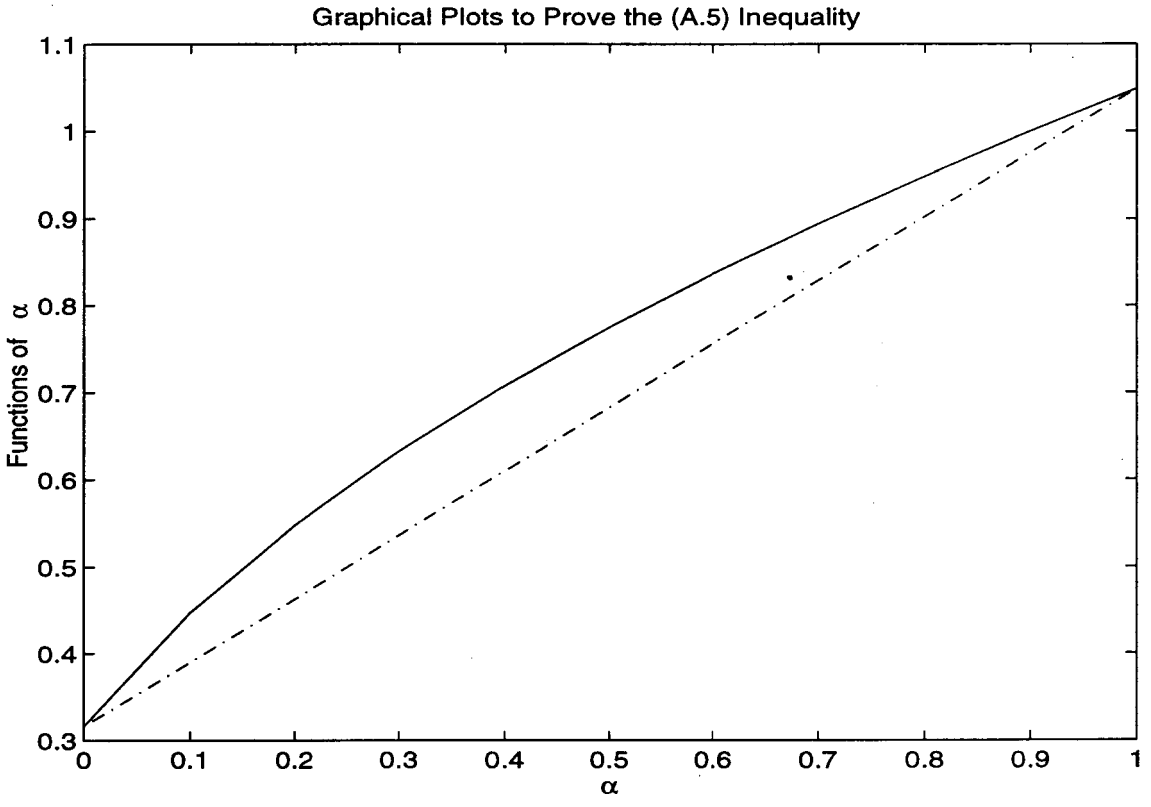

Figure A.1: *The curve is drawn for the function* $f(a) = (.1 + \alpha)^{1/2}$. *The dash-dot line is the chord joining the two end points of the curve. The area under the curve is more than that under the chord. Hence, the positivity of* $d_l(B,m)$ *is proved.*

For the sake of completeness we provide an analytical proof below. It is easy to notice that the difference between the two energies can be written as

$$\Delta E_0(B,m) = E_0(B,m) - E_0(0,m) = \sum_{l=0}^{\infty} d_l(B,m) \tag{A.6}$$

Where $d_l(B,m)$ is given by

$$d_l(B,m) = 2\int_0^1 d\alpha\, \sqrt{z_l+\alpha} - (\sqrt{z_l} + \sqrt{z_l+1}). \tag{A.7}$$

where $z_l = (1+2l\rho)/2\rho$ and $\rho = \frac{eB}{m^2}$ is the dimensionless variable in the problem. Now, ndte that the function $f(a) = \sqrt{z_l+\alpha}$ is convex (see the figure A.1).

Hence, it follows that

$$\int_0^1 d\alpha \sqrt{z_l + \alpha} - \frac{\sqrt{z_l} + \sqrt{z_l + 1}}{2} \geq 0 \tag{A.8}$$

The convergence of this function can be proved easily as before. We note that

$$\int_0^1 d\alpha \, f(\alpha) \leq \left[f(1/2) - \frac{f(0) + f(1)}{2} \right] \tag{A.9}$$

Now, applying mean value theorem twice it is easy to show that

$$\int_0^1 d\alpha \, f(\alpha) \leq \frac{1}{16(z_l + \alpha)} 3/2 \tag{A.10}$$

Notice that the difference between the free energies varies with the cutoff as $\frac{1}{\sqrt{L}}$. This shows that in the relativistic case the response of the vacuum of QED is Diamagnetic in nature which is also in accord with reference [3] where the result obtained depends on the cutoff used in the theory. Our result uses a proper regularization scheme to deduce the diamagnetic behaviour of the renormalized vacuum. If one thinks in terms of virtual pairs of electrons and positrons which have spin, then one would naively believe that the vacuum will be paramagnetic. However, it turns out that it is diamagnetic. This behaviour is well known in the literature [3, 4] and has been explained as a consequence of Pauli exclusion principle. The QED vacuum in an *inhomogeneous* magnetic field as well as with finite chemical potential and finite fermion density has been discussed recently in the literature [5, 6]. The highlight of this appendix is to prove the inequality *exactly* without any approximation.

Bibliography

[1] Joseph I. Kapusta, Finite Temperature Field Theory, (Cambridge, 1989).

[2] K. Deitz, Physica Scripta, T21, 65 (1988).

[3] N. K. Nielsen, **Am.** J. Phys., 49, 1171 (1981).

[4] R. J. Huges, Nucl. Phys. B, 186, 376 (1981).

[5] M. P. Fry, QED in inhomogeneous magnetic fields, preprint hep-ph/9606037; Phys. Rev. D, 53, 980 (1996).

[6] D. Persson and V. Zeitkin, Phys. Rev. D, 51, 2026 (1995); V. Zeitkin, Phys. Lett. B, 352, 422 (1995).

Appendix B

Scaling Exponents a and β from Various Theoretical Models and Experiments

Theoretical	α	β	$\alpha+\alpha/\beta$
1.Eden Model (1961,1985)	0.50 ± 0.01	0.30 ± 0.03	2
2.Restricted Solid on Solid (Kim and Kosterlitz, 1989)	0.50	0.33	2
3.Edwards-Wilkinson model (1982)	0.50	0.25	2.5
4.Kardar-Parisi-Zhang model (1986)	0.50	0.33	2
5.DPD model (Boston Group, 1992,1994)	0.63 ± 0.02		
6.DPD Simulation, moving (Boston Group, 1992,1994)	0.70 ± 0.05	0.70 ± 0.05	1.7
7(a).SOD Model A (Sneppen, 1993)	$1.01 \pm .O1$	0.95 ± 0.05	2.07
7(b).SOD Model B (Sneppen, 1993)	0.63 ± 0.02	0.9 ± 0.1	1.33
8.Cellular Automaton Model (Sunil Kumar and Jana, 1996)	$0.45 - 0.68$	$0.50 - 0.60$	< 2
Experimental	a	β	$\alpha+\alpha/\beta$
1.Paper wetting, pinned (Boston Group, 1992,1994)	0.65 ± 0.05		
2.Paper wetting (Family et.al., 1992)	$0.62 - 0.78$	$0.29 - 0.40$	> 2
3.Paper wetting (Horvath and Stanley, 1995)		0.56 ± 0.03	
4.Paper-towel wetting (Kwon et. al, 1996)	0.67 ± 0.04	0.24 ± 0.02	3.46
5(a).Paper wetting I (Sunil Kumar and Jana, 1996)	0.66 ± 0.02		
5(b).Paper wetting II (Sunil Kumar and Jana, 1996)	0.45 ± 0.05		